MECHANICAL

TECHNOLOGY

INCORPORATED

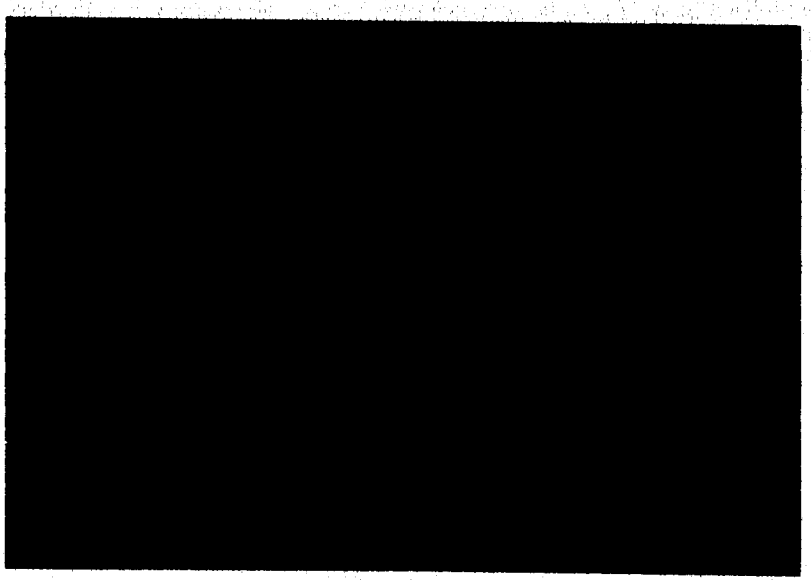

MECHANICAL TECHNOLOGY INCORPORATED
968 Albany-Shaker Road
Latham, New York 12110

MTI-66TR51

SHAKE TABLE TESTS OF A SPIRAL-GROOVED JOURNAL BEARING

by

S.B. Malanoski

February, 1967

No. MTI-66TR51

Date: February, 1967

TECHNICAL REPORT

SHAKE TABLE TESTS OF A SPIRAL-GROOVED JOURNAL BEARING

S. B. Malanoski
Author(s)

H. T. Pan
Approved

Approved

Prepared under

Contract Nonr-3730(00)
Task NR 062-317/4-7-66

Prepared for

Department of Defense
Atomic Energy Commission
National Aeronautics and Space Administration

Administered by

Office of Naval Research
Department of the Navy

MECHANICAL TECHNOLOGY INCORPORATED

968 Albany-Shaker Road—Latham, New York—Phone 785-0922

ABSTRACT

A 1.5 inch diameter, L/D = 1, spiral-grooved, gas journal bearing with a rotor weight of 2-1/8 lb. per bearing, mounted in a housing (total weight of approximately 100 lb.) was subjected to a one (1) g vibrating load over a frequency spectrum of 20 to 2000 cps. Tests were made at rotor speeds of 12,000, 20,000 and 30,000 rpm. The only static bearing load imposed was the rotor weight. The in-line and perpendicular frequency responses of the rotor (both magnitude and phase angle) were measured and recorded. No sign of bearing touchdown was detected. Correlation between this experimental data and available theoretical data was good.

TABLE OF CONTENTS

ACKNOWLEDGEMENTS

The author wishes to thank his colleague, Dr. C.H.T. Pan, for his constructive suggestions, and technical discussions and guidance during the program.

The author is extremely grateful to Mr. P. H. Broussard, Jr. and his associates at Astrionics Laboratory, George C. Marshall Space Flight Center, NASA, Huntsville, Alabama, who not only permitted the use of their shake table test facilities but also contributed much effort in making the present testing program a success.

This work was administerd by Mr. S. W. Doroff, Office of Naval Research, Department of the Navy.

INTRODUCTION

Recently, experiments were made on the spiral-grooved, gas journal bearing to test its steady-state performance (Ref. 1). This bearing performed well when subjected to a steady applied load; i.e., it carried the load at the eccentricity predicted by theory. Also, no sign of bearing whirl instability was detected in the speed range of the investigation.

The next natural step was to test the performance of the same bearing under a vibratory, externally applied load. Under Contract Nonr-3730(00), Task NR 062-317/4-7-66, these tests have been performed and the results are the subject of this report.

A number of reports have been published on the frequency response of a rotor in gas bearings (e.g. Refs. 2, 3 and 4) — all are theoretical in nature. Some theoretical frequency response data has been made available in Reference 2 for the plain infinitely-long bearing. The particular analysis was extended to the finite, plain bearing in Reference 3. Theoretical frequency response data for the plain finite bearing are presented in Reference 4. Also, a further extension of the analysis to the spiral-grooved journal bearing is given with accompanying theoretical results. These theoretical data for the spiral-grooved journal bearing are used in this report for comparison with the now available experimental results.

TEST APPARATUS AND INSTRUMENTATION

The basic elements of the test apparatus are a grooved shaft, two plain bearing sleeves mounted in a housing, two housing end plates incorporating carbon buttons, and a hydrostatic lifter-loader bearing. Its housing has an integral circular base plate so that it can be bolted directly to a shake table with an eight (8) inch bolt circle. The entire weight of the test apparatus is approximately 100 pounds. The 1.5 inch diameter journal, which is 8.75 inches long with 16 turbine blades on one end, is depicted in Figure 1a. Total rotor weight is 4.25 pounds. These two partially-grooved areas running against smooth carbon graphite sleeves comprise the test bearings. These bearings have 36 etched grooves per side, at a spiral angle, $\beta = 25^\circ$. Groove dimensions are 0.021 inches wide, 0.345 inches long and from 500 to 600 microinches deep. The ratio of groove width-to-ridge width is 0.54. At zero speed, the radial clearance is 495 microinches. At 30,000 rpm, the radial clearance has been calculated to be 480 microinches. Therefore, the groove clearance-to-ridge clearance ratio varies from approximately 2.0 to 2.25. The axial length of the grooves takes up 46 percent of the entire bearing length of 1.5 inches, (L/D = 1). Measured between the mid-planes, the bearing span is 5.5 inches. The shaft may be lifted for start-up and shutdown by a hydrostatic lifter-loader bearing, located between the two test bearings. A nozzle ring in conjunction with the 16 blades on the shaft comprise an impulse-type drive turbine. Each end plate has a carbon button, with one button being adjustable. These buttons provide a means for centering the shaft axially and for carrying a slight thrust load when necessary.

The shaft could be driven to a maximum speed of only 34,000 rpm because of the plumbing limitations at the shake table facility. However, the speed was held constant — varying approximately $\pm$ 2 cps during a 7-1/2 minute run. Speed was measured with an optical probe and frequency counter. The optical probe counts a painted pattern on the end of the shaft, and the signal is indicated on the frequency counter.

Temperature of each bearing was recorded by thermocouples embedded in the carbon graphite. The effect of the cool nitrogen blowing past the one bearing as it

escaped from the turbine area could thus be determined. Before each test was made at a given constant speed, the temperatures of both bearings were allowed to reach equilibrium.

The lifter-loader bearing was not used during these tests for applying an external load to the test bearings. Only the rotor weight itself loaded the bearings. At 12,000 rpm, this corresponds to an eccentricity ratio of $\epsilon_o \approx .1$ and at 30,000 rpm, $\epsilon_o \approx .05$. As an extra precaution at start-up and shutdown, a slight pressurization of the lifter-loader bearing was applied to lift the rotor from the test bearings.

The shaft displacement (output) was measured by two horizontal (perpendicular) and two vertical (in-line) capacitance probes. These four capacitance probes were specially fabricated to have a capacitance range of 6 to 30 pico-farads for use with the Photocon-Dynagage* system. Each test bearing has a set of two probes located inboard from the bearing itself and mounted in the housing. An accelerometer was mounted on the housing to measure the G-level of vibration input.

Figures 1b, 1c and 1d illustrate essentially the entire test instrumentation setup.

---

*Capacitance dynamic displacement monitoring equipment manufactured by Photocon Research Products.

EXPERIMENTS

The rotor-bearing housing assembly was mounted on the shake table. (Note Figure 1b). In all tests, the rotor attained a constant speed and the bearings an equilibrium temperature. The bearings communicated with normal atmospheric pressure and temperature.

The first test was a 20-2000 cps log-sweep at one (1) g input vibration level requiring a 7-1/2 minute time duration. The only static load on the bearings was the rotor weight of 4.25 pounds. This test was performed at speeds of 12,000, 20,000 and 30,000 rpm. A paper recording (Visicorder) was made of the in-line and perpendicular displacements of the rotor (output) and of the vibration amplitude of the shake table (input) during the entire test. An oscilloscope was also used to display the rotor in-line displacement versus the shaker input.

At all three speeds, resonances were detected at, or near, "half-frequency" and at a higher frequency which varied from 550 to 700 cps — depending on the rotor speed. Discrete frequency tests were then made with a slower recorder paper speed at these resonant frequencies in order to study in detail the phase relation between the input and output, and to obtain a more accurate response magnitude reading. Both in-line and perpendicular responses were studied.

The final test was a 1-g rms flat-spectrum, random input test at 12,000 rpm. The in-line response of the rotor at one bearing position was recorded on tape and these results were then analyzed to obtain a "power spectral density" plot.

DISCUSSION OF EXPERIMENTAL RESULTS

Figures 2, 3, and 4 give a comparison of theory and experiment for the in-line and perpendicular frequency response magnitude for three rotor speeds of 12,000 20,000 and 30,000 rpm respectively. The continuous solid line is the theory, (Ref. 4)and the points symbolized by (x and •) are the experimental points for the two specific bearings. One can note the generally good correlation between theory and experiment. There are two resonant frequencies; one at or near 1/2 frequency, the other in the high frequency range of from 550 to 700 cps. The in-line response magnitudes at these two resonances are about equal at 12,000 rpm. At the higher rotor speed of 20,000 rpm, the 1/2 frequency resonant magnitude is considerably reduced and at still a higher rotor speed of 30,000 rpm, this response is hardly noticeable. On the other hand, the magnitude of the high frequency resonance is not effected by the increase in speed, i.e., it remains rather constant at around 7 (or 8) to 1. The perpendicular response magnitude is comparatively small (15 percent of the in-line response magnitude) at the high frequencies including the resonant frequency, but at 1/2 frequency the perpendicular response magnitude is approximately 65 percent of the in-line response. Notice the stiffening effect of increasing the rotor speed by examining the low frequency in-line response. At 12,000 rpm the response is 2.9 to 1, at 20,000 rpm the response is 2.3 to 1, and at 30,000 rpm, 1.3 to 1. In addition, notice that there is essentially no measurable response at frequencies above the high frequency resonance.

Figure 5 can be used to examine the phase relationship between the input and output, (rotor response). This figure consists of three samplings of the Visicorder. Each sampling consists of five distinct recordings. From left to right: the first two correspond to the in-line response (two bearings); the second two correspond to the perpendicular response; and the fifth recording is the input to the shake-table and bearing housing. The horizontal line is a timing line. The theory, (Ref. 4), predicts that the in-line response should be in phase with the input and the perpendicular response should be 90° lagging at the 1/2 frequency resonance. Indeed, this is borne out by the experimental data shown by the first two samplings, 5a and 5b, corresponding to rotor speeds of 12,000 rpm and 30,000 rpm respectively.

The theory further predicts that both the in-line and perpendicular responses should be 90° lagging at the high frequency resonance. The third recorder sampling, Figure 5c, shows the in-line response to be lagging by approximately 90° at 560 cps. The perpendicular response is small and overshadowed by the background noise of instrumentation and one cannot determine the phase relationship.

An interesting observation was made on the oscilloscope at half frequency at all rotor speeds. The "scope" picture was elliptical in nature and contained an orbiting bright spot. Just under half frequency, the bright spot rotated in one direction; right at half frequency the spot was stationary; just above half frequency the bright spot rotated in the opposite direction. Perhaps one might use this information to determine the exact rotor speed without using a frequency meter.

In Figure 6, a series of oscilloscope photographs are given which illustrate the in-line response of the rotor (vertical axis) versus the input to the housing (horizontal axis) for a frequency range of from 90 cps (just under 1/2 frequency) to 700 cps at a rotor speed of 12,000 rpm. These figures are perhaps best understood if one considers the following:

Let the input (x-axis) be represented by $x = a \cos \omega t$, and the output (y-axis) by $y = b \cos (\omega t - \phi)$. These two parametric equations are equivalent to the one equation for an ellipse, $(\frac{x}{a})^2 - 2 (\frac{x}{a})(\frac{y}{b}) \cos \phi + (\frac{y}{b})^2 = \sin^2 \phi$. In this equation, ϕ is the phase angle between the input and in-line rotor response (output). From the theory, we already know that this phase angle is zero at the "half frequency" resonance, $\phi = -90°$ at the high frequency resonance and $\phi = -180°$ at frequencies above this high frequency resonance. Now consider the photographs in Figure 6. If $\phi = 0°$ or $-180°$, the above equation reduces to straight-line equations $\frac{y}{b} = \frac{x}{a}$, and $\frac{y}{b} = -\frac{x}{a}$ respectively. Note that at 90 cps, the photograph is a straight line with a positive slope and at 700 cps, the photograph is a straight line with a negative slope. This indicates that the half frequency resonance is slightly below 100 cps, or about 90 cps, and that the higher

resonant frequency lies below 700 cps. If $\phi = -90°$, the above equation reduces to a principal ellipse — refer to the photographs at 560 cps and 600 cps. The photographs for 110 cps and 200 cps illustrate that ϕ has some value other than $0°$, $\pm 90°$ or $\pm 180°$. In theory, $\phi \approx -10°$ at 110 cps and $\phi \approx -45°$ at 200 cps.

Figure 7 illustrates the results of a 1g rms flat spectrum random input test at 12,000 rpm. Measurement of the magnitude of the in-line rotor response was made at one bearing position. The results (power spectral density) indicate that the majority of the "power" is at the two resonances approximately 100 cps and 650 cps. This confirms what has been observed and discussed above; for example, Figure 2, 3 and 4. Generally speaking, the system behaves more or less like a lightly damped linear system — but with two resonances.

During these tests, the temperature at each bearing location was measured. This allowed one to determine the equilibrium temperature at each running speed before the dynamic load was applied. These temperatures are tabulated below:

Speed, rpm	Turbine End, Bearing	Speed Pick-Up End, Bearing
0	83.25°F	83.25°F
12,000	85.2° F	86.9° F
20,000	91.8° F	95.0° F
30,000	94.5° F	104.9° F

The effect of the cooling turbine-drive gas is indicated in the above table. The temperature difference between bearings is 10°F at 30,000 rpm. Thus, the viscosity difference and axial thermal distortions along the rotor are essentially negligible. It should be further noted that the temperature at each bearing rose gradually, the total rise being typically 1°F during a 7-1/2 minute vibration test.

CONCLUSIONS AND RECOMMENDATIONS

A simple rotor, rotating at speeds of 12,000, 20,000 and 30,000 rpm, in lightly-loaded, spiral-grooved journal bearings has been subjected to a 1 g vibratory load from 20 to 2000 cps and performed as predicted by previously available theoretical data; i.e.,

a) Two resonances occurred - one near 1/2 frequency and one at a much higher frequency.

b) The magnitude of both the in-line and perpendicular frequency response at 1/2 frequency decreased with increasing speed. This is an improvement over plain bearing performance.

c) The in-line magnitude of the high frequency resonance remained rather constant within the speed range tested. The corresponding perpendicular response was essentially negligible.

d) The resonant frequency conditions could be easily pin-pointed by observing the oscilloscope picture of the in-line frequency response versus the shaker input.

e) At frequencies above the high frequency resonance the response is negligible.

A "power spectral density" plot was made of the in-line response magnitude to a random 1 g rms vibration at a rotor speed of 12,000 rpm. The plot shows maximum power at 100 cps and 650 cps, corresponding to the half-frequency and high frequency resonance, respectively.

It is recommended that this same rotor-bearing system be tested at higher rotor speeds and perhaps larger g — levels.

It is further recommended, that at higher speeds — near 45,000 rpm, the rotor-bearing system be monitored very closely for observation of the critical speed of the rotor. See Appendix for a discussion on rotor critical speed.

REFERENCES

1. Malanoski, S. B., "Experiments on an Ultrastable Gas Journal Bearing", Trans. ASME, Paper No. 66-Lub-6, Presented at the ASME-ASLE Lubrication Conf., Minneapolis, Minn., October 18-20, 1966.

2. Ausman, J. S., "On the Behavior of Gas-Lubricated Journal Bearings Subjected to Sinusoidally Time-Varying Loads", Trans. ASME, Journal of Basic Engineering, Vol. 87, Series D, No. 3, pp. 589, 598, September 1965.

3. Pan, C.H.T., and Malanoski, S. B., Discussion of Ref. 2, Trans. ASME, Journal of Basic Engineering, Vol. 87, Series D, No. 3, pp. 599-602, September 1965.

4. Malanoski, S. B., and Dougherty, D. E., "Journal Bearing Dynamic Response", ONR Report-MTI No. 66TR48, prepared under contract Nonr-3730(00), Task NR062-317/4-7-66, Administered by Office of Naval Research, Dept. of the Navy, February 1967.

5. Pan, C.H.T., and Sternlicht, B., "On the Translatory Whirl Motion of a Vertical Rotor in Plain Cylindrical Gas Dynamic Journal Bearings", Trans. ASME, Journal of Basic Engineering, Vol. 84, Series D, No. 1, March 1962.

NOMENCLATURE USED WITH FIGURES

$\Lambda = \frac{6\mu\omega}{p_a} \left(\frac{R}{C}\right)^2$ Bearing Number:

μ - absolute viscosity of gas, psi-sec

ω - angular velocity of rotor, rad/sec

p_a - ambient pressure, psia

R - radius of shaft, in.

C - radial clearance, in.

L/D Slenderness Ratio:

L - bearing length, in.

D - bearing diameter, in.

$\Omega = \frac{MC\omega^2}{2LDp_a}$ Mass Parameter:

M - mass of rotor per bearing, $lb.sec^2/in.$

$\epsilon_o = e/C$ Eccentricity Ratio:

e - radial displacement of shaft, in.

$\frac{\epsilon_t}{N_t} = \frac{2DLp_a}{C} \frac{e_t}{V}$ Response Magnitude:

e_t - displacement due to dynamic load, in.

V - mG

m - rotor weight per bearing, lb.

G - a/g; number of G's acceleration

Groove Parameters:

a_g/a_r - Groove width/ridge width
h_g/h_r - Groove clearance/ridge clearance
β - Spiral angle, deg.
$\bar{Y}$ - Total groove axial length/bearing length

$f = \frac{\dot{\alpha}}{\omega}$ Frequency Ratio:

$\dot{\alpha}$, vibration frequency or whirl frequency, rad/sec

δ/e Displacement Ratio:

δ, distance between rotor mass center and rotor geometric center, in.

APPENDIX

Rotor Critical Speed

The rotor critical speed may be determined from the following equation and condition: (See Ref. 5 for derivation).

$$\left(\frac{K_r}{m\omega^2 \cos\phi}\right)^2 - \frac{2K_r}{m\omega^2} + 1 = \left(\frac{\delta}{e}\right)^2 \qquad (A.1)$$

Minimization of $\frac{\delta}{e}$ represents the point of the rotor critical speed.

K_r = dynamic radial stiffness associated with synchronously whirling rotor, lb./in.

m = mass of rotor per bearing, $lb.sec^2/in.$

ϕ = dynamic attitude angle, deg.

ω = rotor rotating speed equal to whirling speed, rad/sec.

δ = distance between rotor mass center and rotor geometric center, in.

e = bearing eccentricity, in.

For the present rotor-bearing system the value of $\frac{\delta}{e}$ calculated according to Eq. (A.1) has been plotted versus the rotor speed in Fig. 8. Notice it reaches a minimum value between 42,000 and 48,000 rpm. Plotted on the same graph is the vibration frequency ratio, f, associated with the maximum amplitude of the in-line rotor response at the higher resonance condition. Note that this curve has a frequency ratio of f = 1 at approximately 45,000 rpm. These two methods thus predict the rotor critical speed at 45,000 rpm.

In Ref. [1] it was reported that this rotor critical speed could not be observed on the oscilliscope. This inability to observe the synchronous whirl orbit was due to two reasons:

(1) the gradual behavior of the δ/e versus speed curve at its minimum, (See Fig. 8) and

(2) the calculated value of the synchronous whirl orbit is less than 5 micro-in. based on $\delta/e = \frac{1}{4}$, (Fig. 8) and a measured unbalance of 40 micro-ounce-in. This is less than the oscilliscope, total reading error of 10 micro-in.

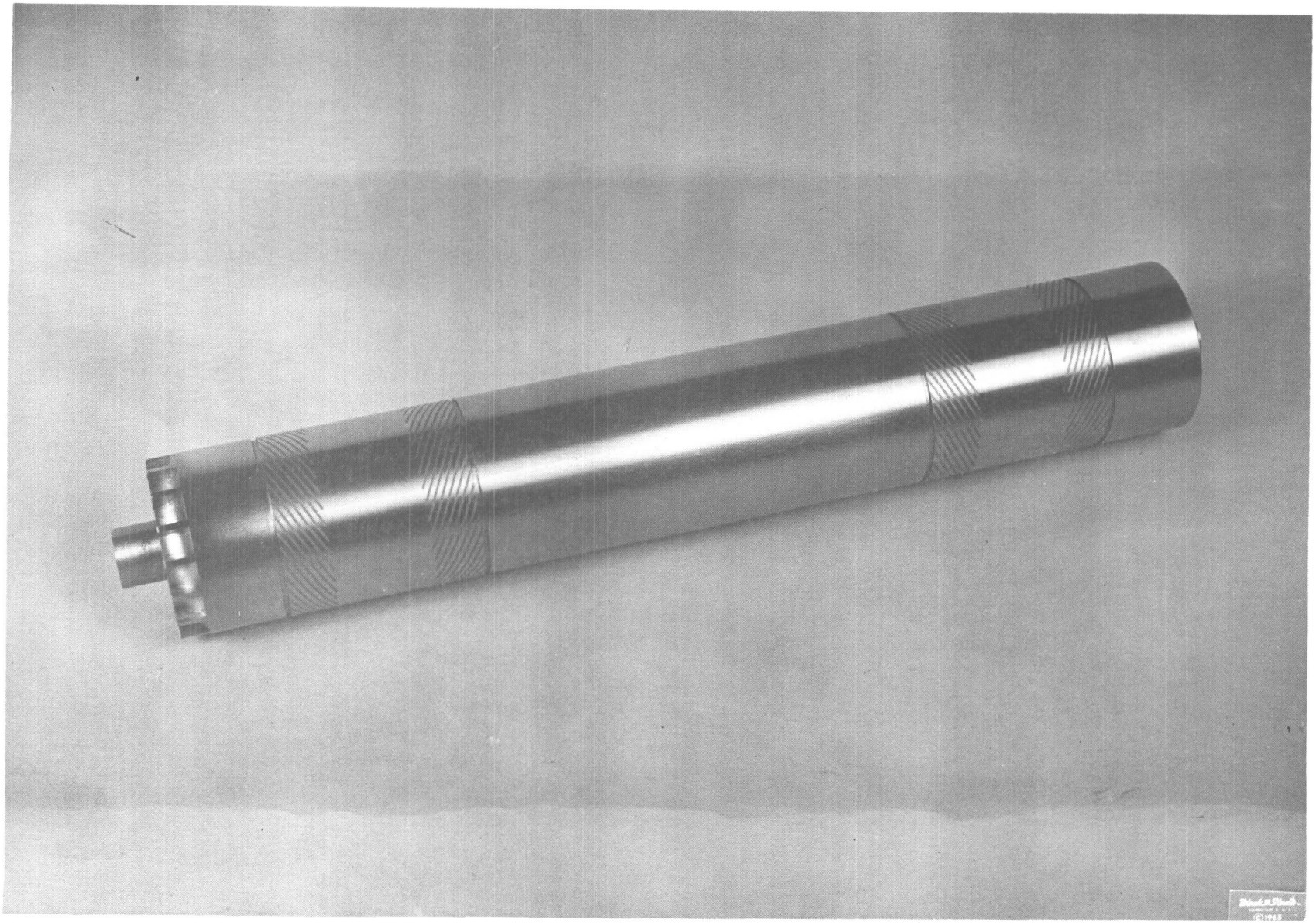

Fig. 1a Test Shaft Illustrating Spiral Grooving and Turbine Blades

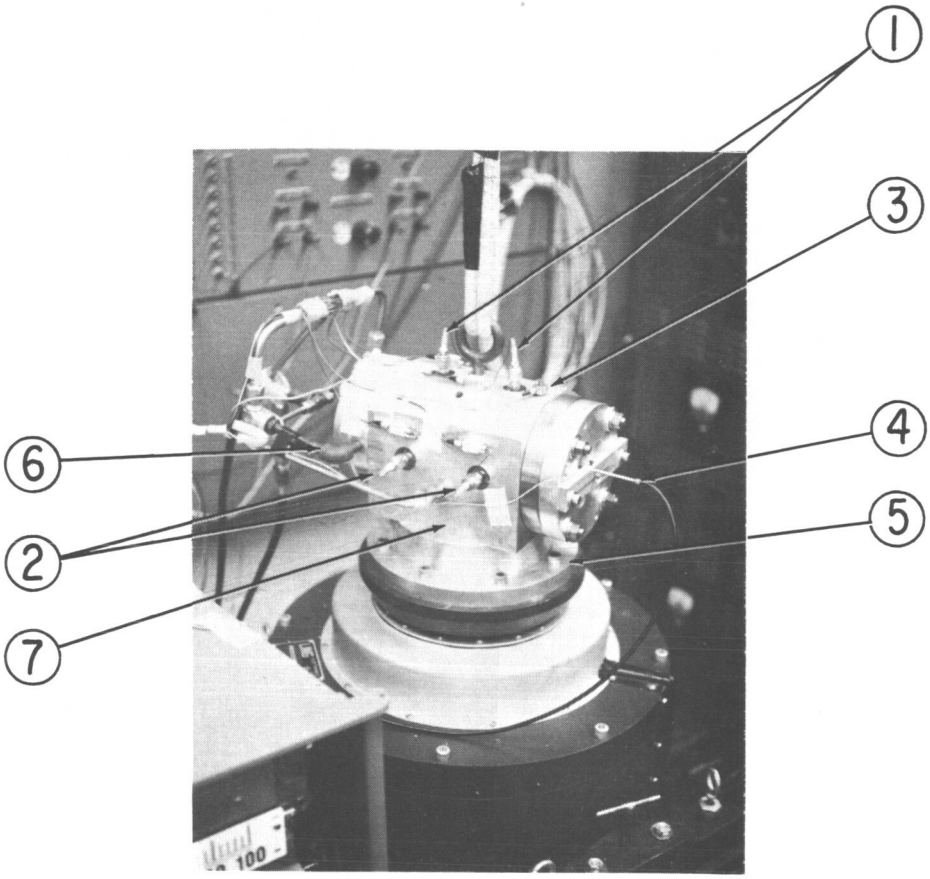

1. In-line (vertical) Capacitance probes.
2. Perpendicular (horizontal) Capacitance probes.
3. Accelerometer for measuring G-level of shake table input.
4. Light Probe for measuring fluctuation of an alternately painted shaft end.
5. Base plate of housing indicating attachment with shake table.
6. Compressed Gas Inlet to Turbine Drive.
7. Housing enclosing test Rotor and Bearing.

Fig. 1b Close-up of Test Rig

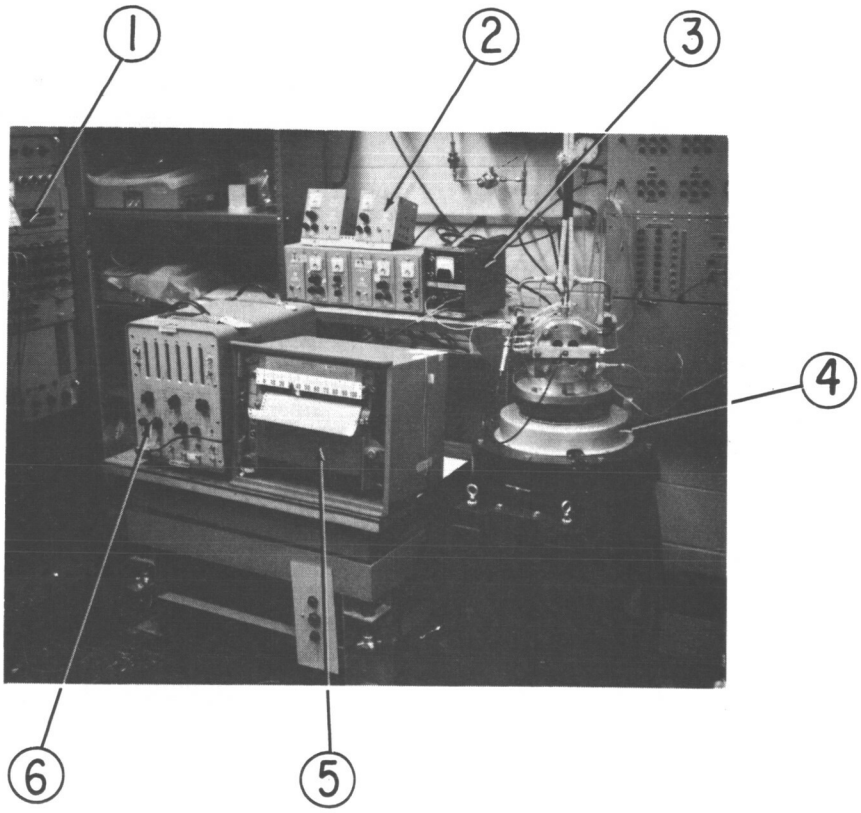

1. VISICORDER FOR INDICATING DISPLACEMENT OF ROTOR WITH RESPECT TO FIXED BEARING.
2. PHOTO-CON MEASURING EQUIPMENT FOR PICKING UP CAPACITANCE PROBE SIGNAL THROUGH A TRANSDUCER.
3. FOTONIC SENSOR USED TO SUPPLY FREQUENCY COUNTER WITH VOLTAGE CHANGE.
4. SHAKE-TABLE.
5. PAPER RECORDER FOR INDICATING TEMPERATURE OF BEARINGS.
6. FREQUENCY COUNTER FOR INDICATING SHAFT SPEED.

Fig. 1c Overall View of Instrumentation

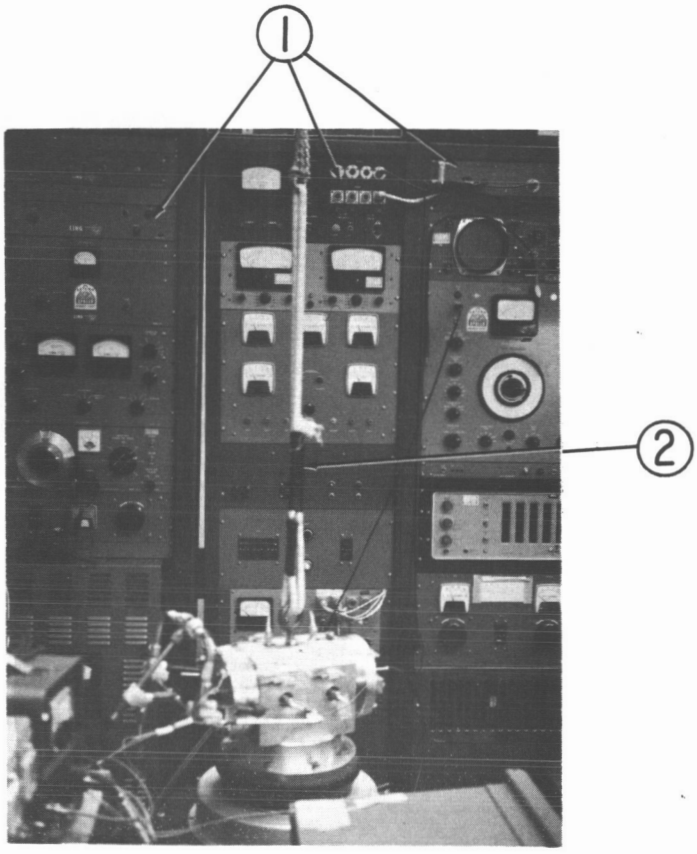

1. Ling Electronic Shake-Table Equipment Console.
2. Low Stiffness Spring Used to Relieve Housing Dead Weight load from Shake-Table.

Fig. 1d Close-up of Shake Table Console

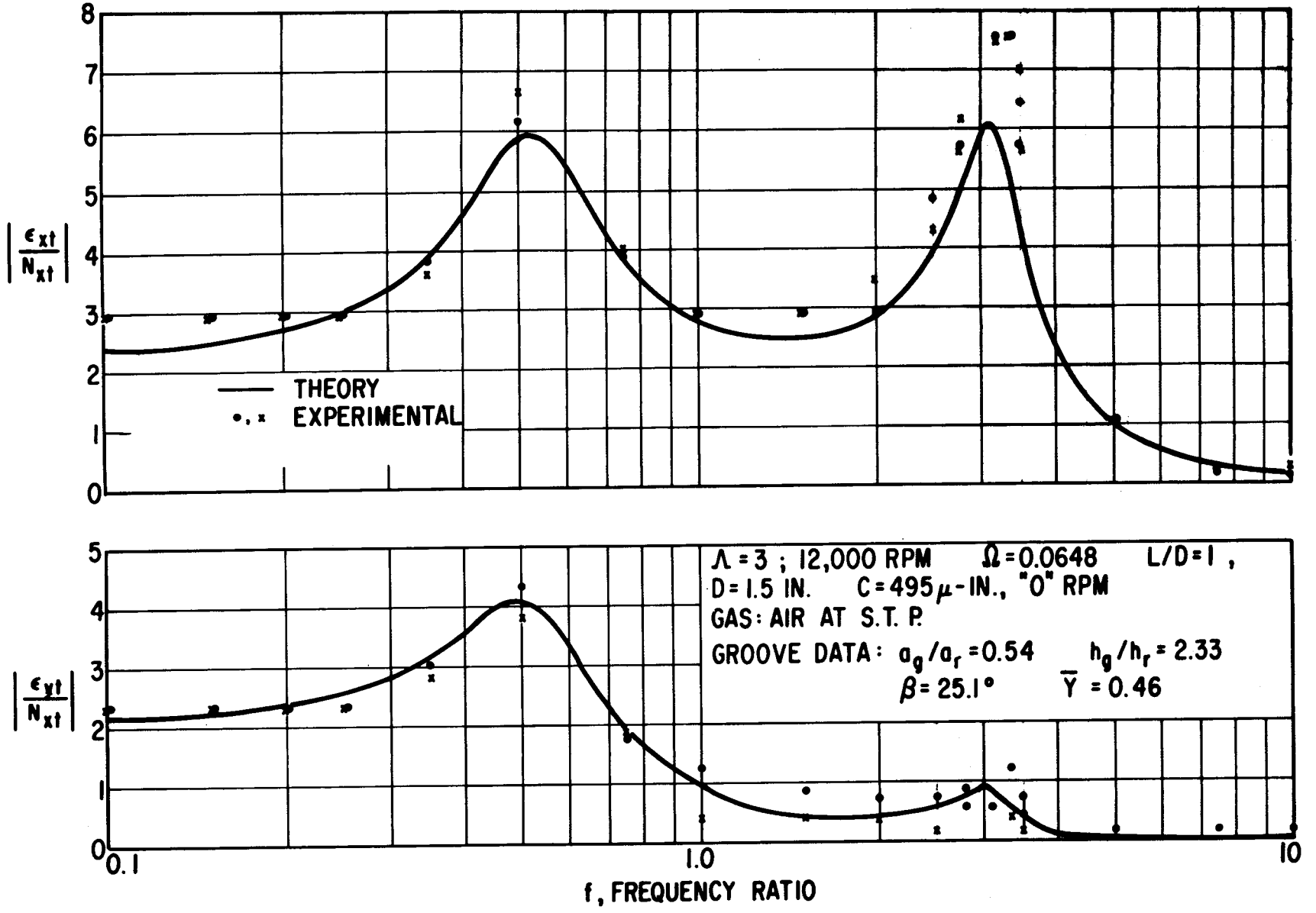

Fig. 2 In-line and Perpendicular Frequency Response, Magnitude Comparison of Theory and Experiment, Λ = 3, 12,000 rpm.

MTI-3443

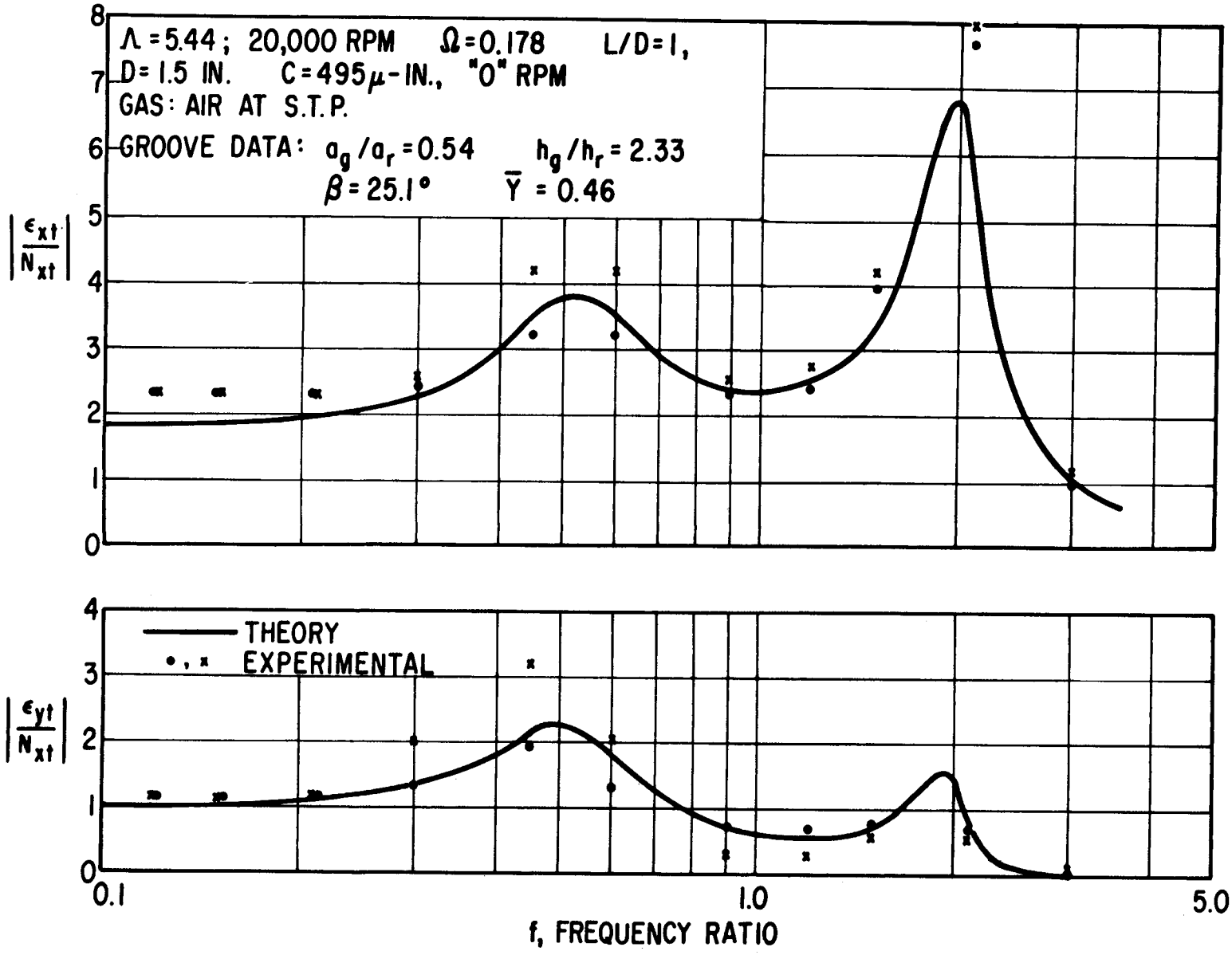

Fig. 3 In-line and Perpendicular Frequency Response, Magnitude Comparison of Theory and Experiment, $\Lambda = 5.44$, 20,000 rpm.

MTI-3448

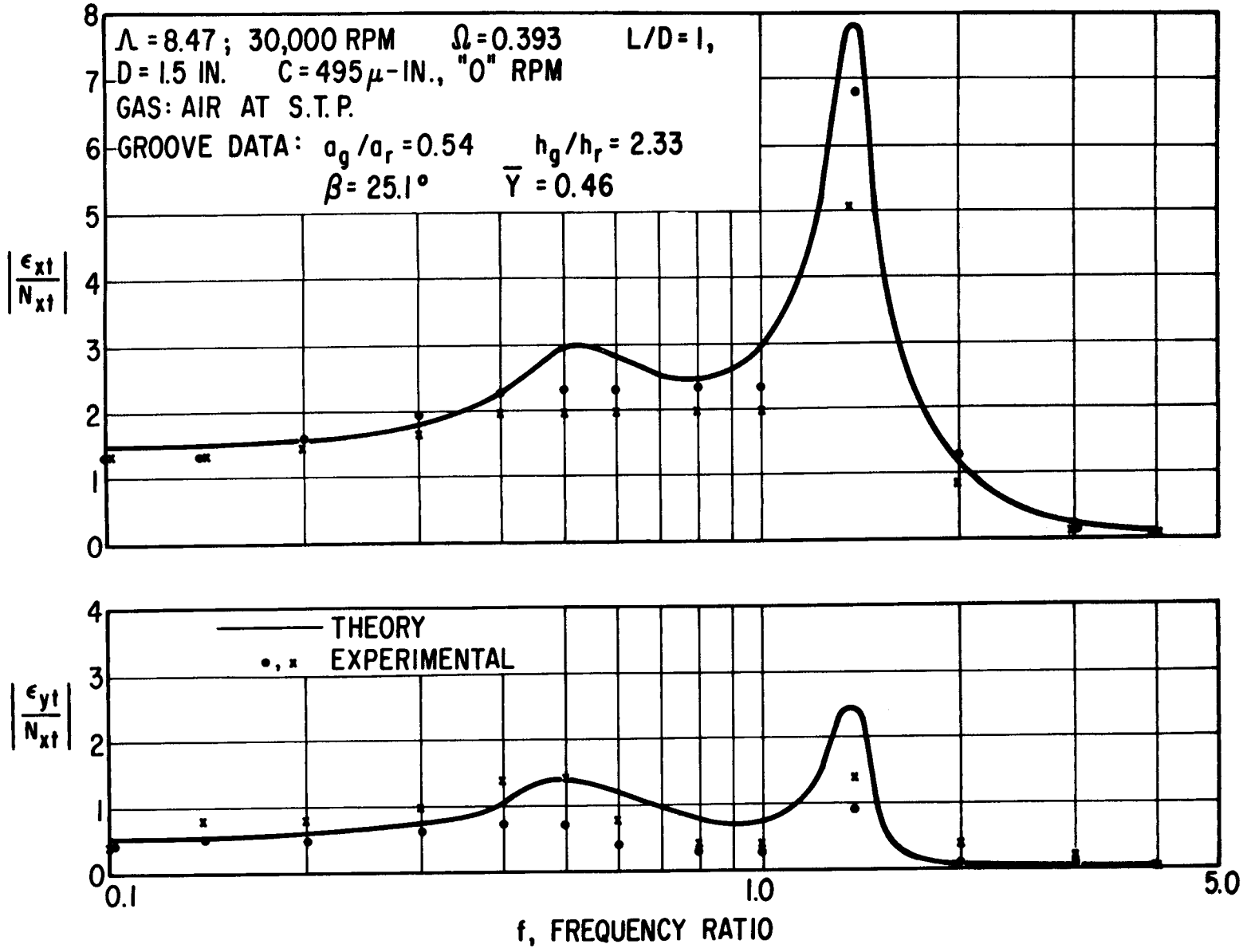

Fig. 4 In-line and Perpendicular Frequency Response, Magnitude Comparison of Theory and Experiments, Λ = 8.47, 30,000 rpm.

MTI-3447

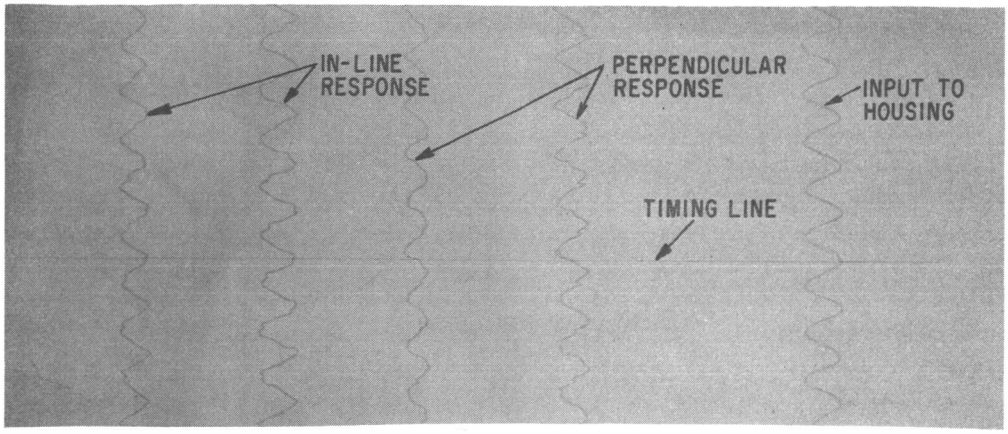

12,000 RPM ROTOR SPEED 100 CPS VIBRATION FREQUENCY (75 % SIZE)

Fig. 5a Recorder Output Sampling Showing Phase Angle of X and Y Output at f ~ 1/2, 12,000 rpm.

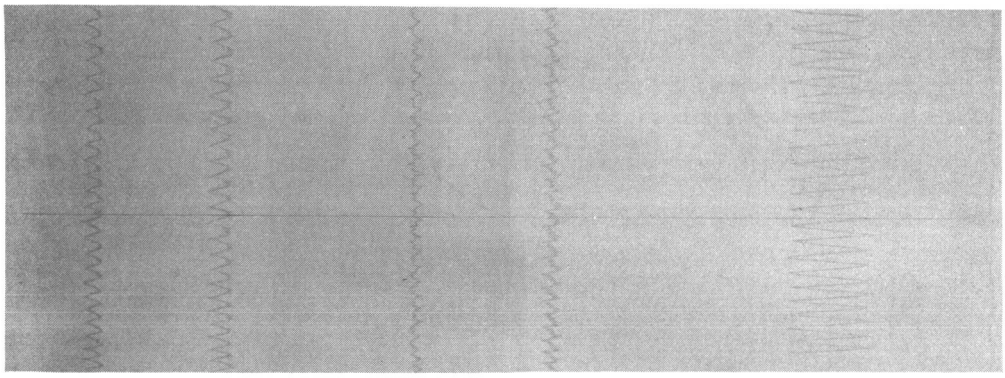

30,000 RPM ROTOR SPEED 250 CPS VIBRATION FREQUENCY

Fig. 5b Recorder Output Sampling Showing Phase Angle of X and Y Output at f ~ 1/2, 30,000 rpm.

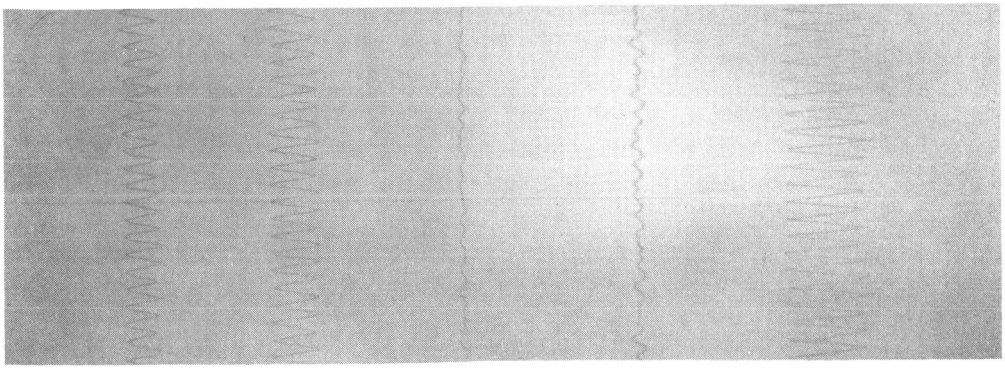

12,000 RPM ROTOR SPEED 560 CPS VIBRATION FREQUENCY

Fig. 5c Recorder Output Sampling Showing Phase Angle of X and Y Output Near High Frequency Resonance, 12,000 rpm.

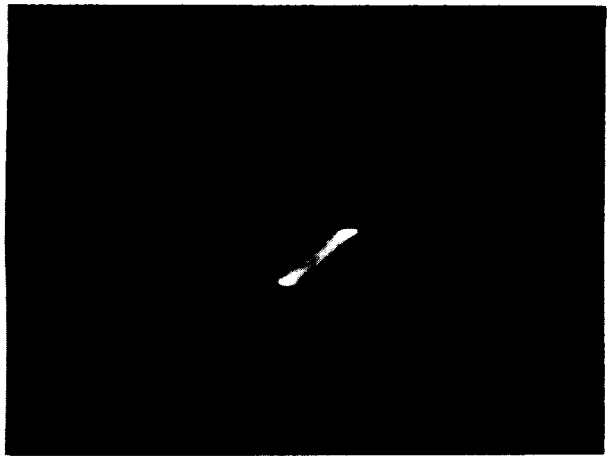

(a)

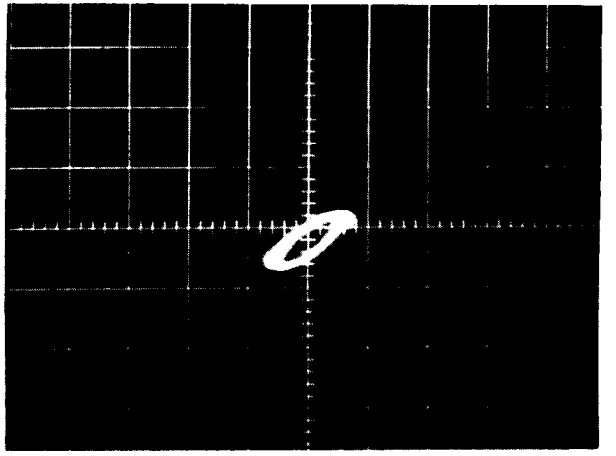

(b)

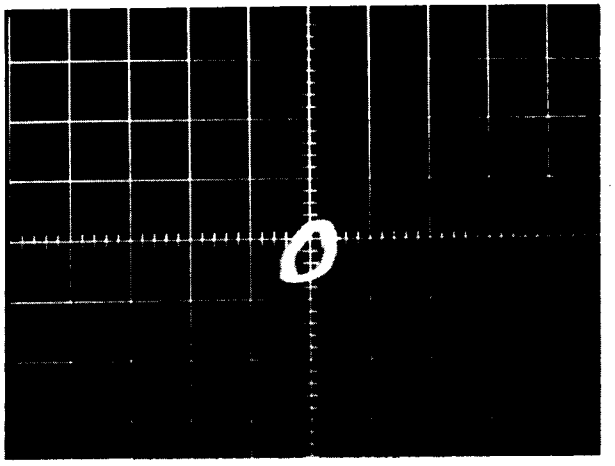

(c)

	VIBRATION FREQUENCY CPS	ROTATIONAL SPEED RPM
(a)	90	12,000
(b)	110	12,000
(c)	200	12,000

Fig. 6 A Series of Oscilloscope Pictures (output versus input) from Vibration Frequencies of 90 cps to 700 cps at Rotor Speed of 12,000 rpm.

MTI-3446

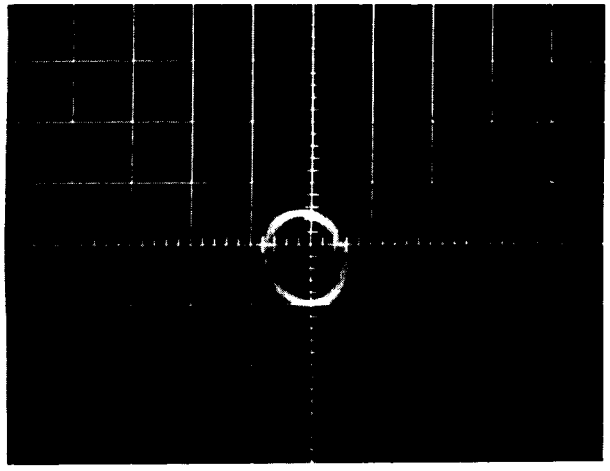

(d)

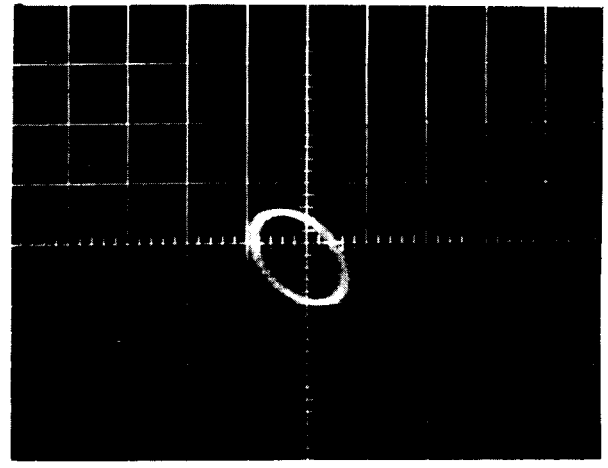

(e)

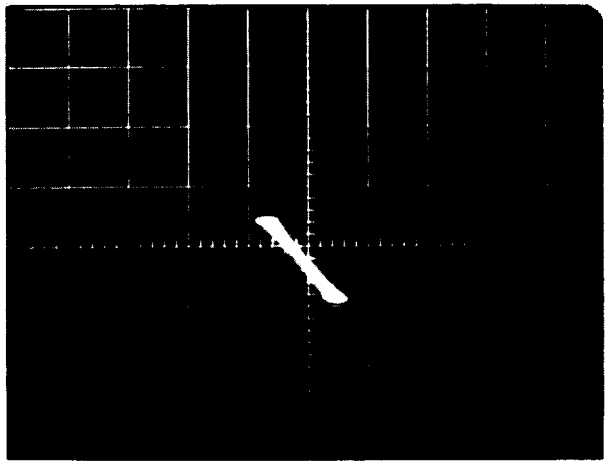

(f)

	VIBRATION FREQUENCY CPS	ROTATIONAL SPEED RPM
(d)	560	12,000
(e)	600	12,000
(f)	700(-)	12,000

Fig. 6 A Series of Oscilloscope Pictures (output versus input) from Vibration Frequencies of 90 cps to 700 cps at Rotor Speed of 12,000 rpm.

MTI-3445

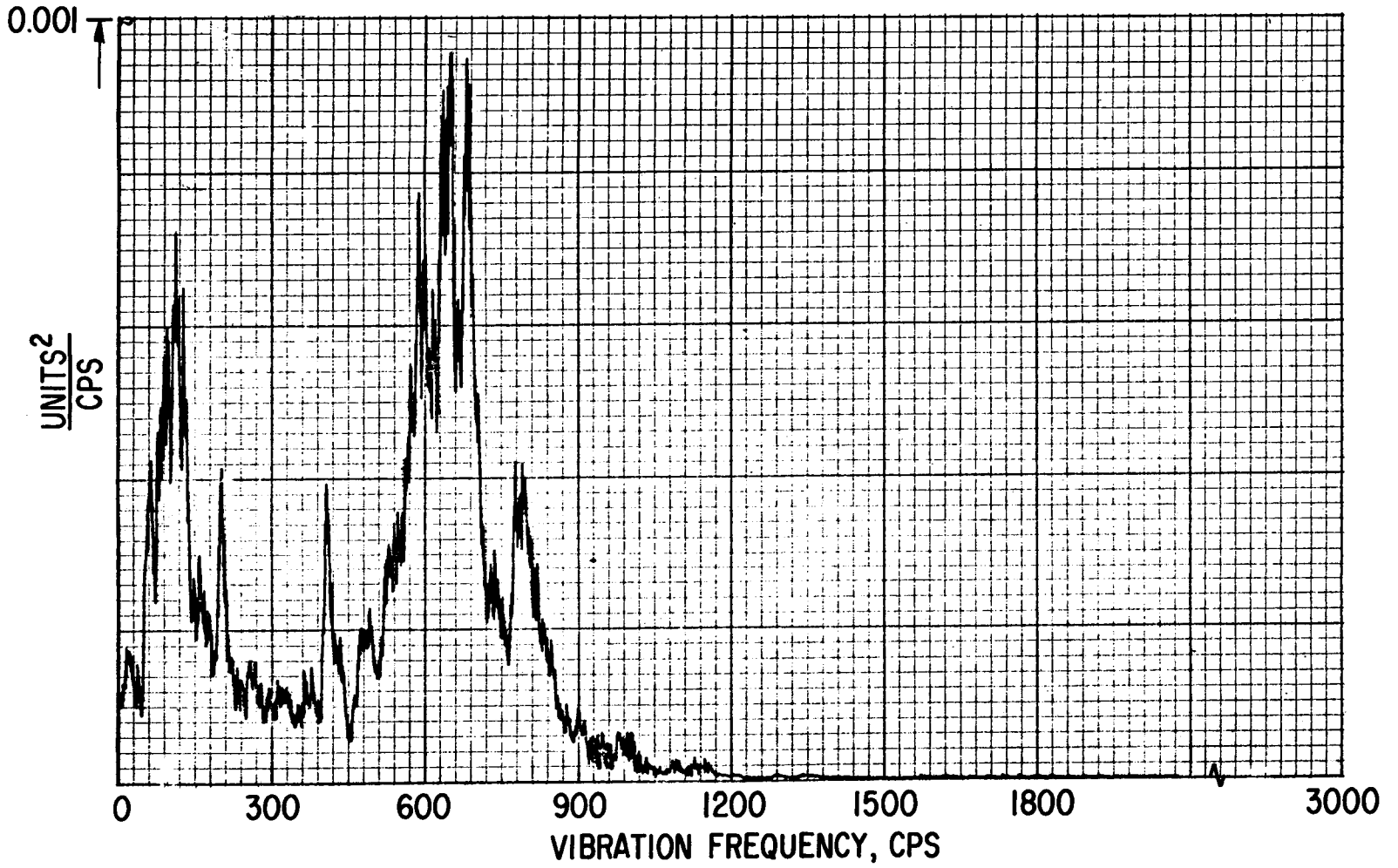

Fig. 7 Power Spectral Density of the In-line Displacement at Turbine End of Shaft, 12,000 rpm, 1-g_{rms} input "flat" from 20 to 2000 cps.

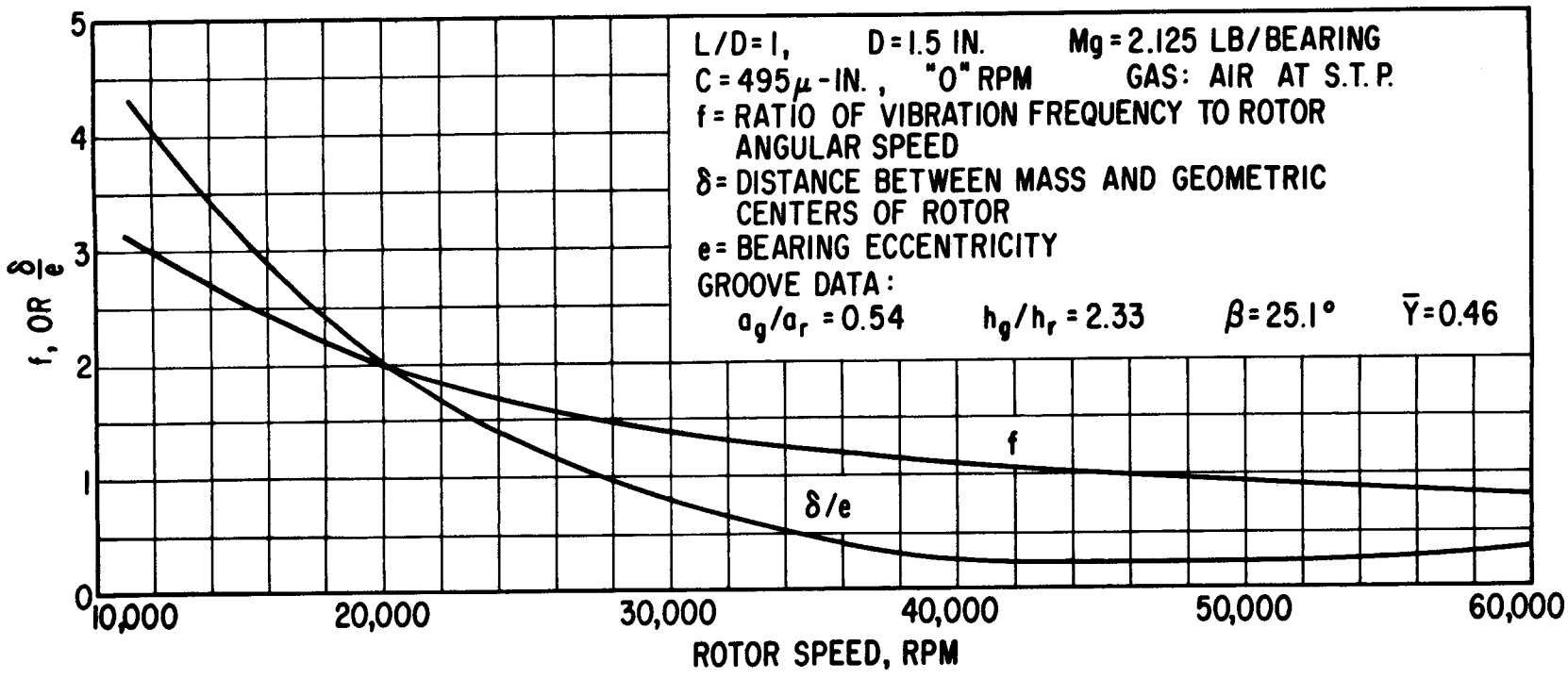

Fig. 8 $\dot{\alpha}/\omega$ and δ/e versus Rotor Speed

APPROVED DISTRIBUTION LISTS FOR UNCLASSIFIED TECHNICAL REPORTS
ISSUED UNDER
GAS LUBRICATED BEARINGS CONTRACTS

Contract Nonr 3730(00) NR 062-317

(ONR-4)

Chief of Naval Research
Department of the Navy
Washington 25, D.C. 20360 (3)
Attn: Code 438
429
463

Commanding Officer
Office of Naval Research
Branch Office
495 Summer Street
Boston, Massachusetts 02110

Commanding Officer
Office of Naval Research
Branch Office
279 South Dearborn Street
Chicago, Illinois 60604

Commanding Officer
Office of Naval Research
Branch Office
207 West 24th Street
New York, New York 10011

Commanding Officer
Office of Naval Research
Branch Office
Box 39
Fleet Post Office
New York, New York 09510 (25)

Commanding Officer
Office of Naval Research
Branch Office 1030 East Green Street
Pasadena, California 91101

Commanding Officer
Office of Naval Research
Branch Office
1076 Mission Street
San Francisco, California 94103

Commander
Naval Ship Systems Command
Washington, D.C. 20360
Attn: 6644 C (R. M. Petros)

Department of the Navy
Naval Air Systems Command
Washington, D.C. 20360
Attn: (S. M. Collegeman)
(M. R. Walters)

Director
Naval Research Laboratory
Washington, D.C.
Attn: Code 2027
5230 (6)

Special Projects Office
Department of the Navy
Washington 25, D.C.
Attn: Code SP230 (D. Gold)
SP001 (Dr. J.P. Craven)

Commanding Officer and Director
U.S. Navy Marine Engineering Laboratory
Annapolis, Maryland
Attn: Code 800
Code 852 (Watt V. Smith)

Superintendent
U.S. Naval Postgraduate School
Monterrey, California
Attn: Library

Commanding Officer
U.S. Naval Avionics Facility
Indianapolis 18, Indiana
Attn: J. G. Weir RDM-4

Commanding General
U.S. Army Material Command
Research & Development Directorate
Research Division
Washington, D.C. 20315
Attn: Mr. Norman L. Klein

Chief of Research and Development
Office of Chief of Staff
Department of the Army
The Pentagon, Washington, D.C. 20310

Commanding General
U.S. Army Engineer R & D Laboratories
Fort Belvoir, Virginia 22060
Attn: W. M. Crim,
Field Office
Technical Documents Center

Redstone Scientific Information Center
Attn: Chief, Document Section
U.S. Army Missile Command
Redstone Arsenal, Alabama 35809

Commanding Officer
U.S. Army Research Office
ESD - AROD
Box CM, Duke Station
Durham, North Carolina 27706

Chief of Staff
U.S. Air Force
The Pentagon
Washington, D.C. 20330
Attn: AFRDR-AS/M

Commander
Air Force Office of Scientific Research
Washington, D.C. 20333
Attn: SRHM

Commander, R & T Division
Air Force Systems Command
Attn: L.M. Medgepeth (APIP-1)
R.W. McAdory (AVNE)
Wright-Patterson AFB, Ohio 45433

AF Flight Dynamics Laboratory
Attn: Mr. W. C. Buzzard (FDFM)
Wright-Patterson AFB, Ohio 45433

Air Force Aero Propulsion Laboratory
Attn: APFL (Mr. John L. Morris)
Wright-Patterson AFB, Ohio 45433

Mr. Lukasiewicz
Chief, Gas Dynamics Facility
Arnold Air Force Station
Tennessee 37389

Mr. Clarence E. Miller, Jr.
Division of Reactor Development & Technology
U.S. Atomic Energy Commission
Washington, D.C. 20545 (2)

Mr. N. Grossman, Chief
Engineering Development Branch
Reactor Development Division
U.S. Atomic Energy Commission
Washington, D.C. 20545 (2)

Headquarters Library
U.S. Atomic Energy Commission
Washington, D.C. 20545

U.S. Atomic Energy Commission
Oak Ridge Operations Office
P.O. Box E
Oak Ridge, Tennessee 37831
Attn: Charles A. Keller

U.S. Atomic Energy Commission
Portsmouth Area Office
Piketon, Ohio 45661
Attn: Dr. Malone

Chief, Division of Engineering
Maritime Administration
441 G Street, N.W.
Washington, D.C. 20235

Cryogenic Data Center
National Bureau of Standards
Boulder, Colorado 80302

Director, Lewis Research Center
National Aeronautics & Space Administration
Attn: Mr. E. E. Bisson
Cleveland, Ohio 44871

NASA Scientific & Technical Information Facility
Attn: Acquisitions Branch (SAK/DL)
P. O. Box 33
College Park, Maryland 20740

Defense Documentation Center
Cameron Station
Alexandria, Virginia 22314 (20)

NASA Lewis Research Center
Attn: Library MS 60-3
21000 Brookpark Road
Cleveland, Ohio 44135

Mr. P. H. Broussard, Jr.
Guidance and Control Division
National Aeronautics and Space Administration
George C. Marshall Space Flight Center
Huntsville, Alabama 35812

United States Atomic Energy Commission
Div. of Technical Info. Extension
P. O. Box 62
Oak Ridge, Tennessee 37830

Aerojet-General Nucleonics
P. O. Box 86
San Ramon, California 94583

Aerospace Corporation
P. O. Box 95085
Los Angeles, California 90045
Attn: Library, Reports Acquisitions Group

AiResearch Manufacturing Company
P. O. Box 5217
Phoenix, Arizona 85010
Attn: Mrs. J.F. Mackenzie, Librarian

American Institute of Aeronautics and Astronautics
Technical Information Service
750 Third Avenue
New York, New York 10017

American Society of Lubrication Engineers
838 Busse Highway
Park Ridge, Illinois 60068

Otto Decker, Manager
Friction & Lubrication Lab
Franklin Institute
20th and Parkway
Philadelphia, Pennsylvania 19103

Dr. W. A. Gross
Ampex Corporation
401 Broadway
Redwood City, California 94063 (2)

Mr. Stanley L. Zedekar
Department 244-2, Building 71
Autonetics
P. O. Box 4181
Anaheim, California 92803

C. C. Flanigen
Director of Engineering
Lycoming Division, Avco Corporation
Stratford, Connecticut 06497

Dr. Russell Dayton
Battelle Memorial Institute
505 King Avenue
Columbus, Ohio 43201

Walt Tucker
Nuclear Engineering Department
Brookhaven National Laboratory
Upton, Long Island, New York 11973

Jet Propulsion Laboratory
California Institute of Technology
4800 Oak Grove Avenue
Pasadena, California 91103
Attn: Library

Dr. F. Osterle
Mechanical Engineering Department
Carnegie Institute of Technology
Pittsburgh, Pennsylvania 15213

Professor M. C. Shaw, Head
Department of Mechanical Engineering
Carnegie Institute of Technology
Pittsburgh, Pennsylvania 15213

Dr. W. T. Sawyer
Department of Mechanical Engineering
Catholic University
Washington, D.C. 20017

Mr. George H. Pedersen
Curtiss-Wright Corporation
Wright Aeronautical Division
Woodridge, New Jersey 07075

Robert H. Josephson, Manager
Clevite Corporation
Mechanical Research Division
540 East 105th Street
Cleveland, Ohio 44108

Professor V. Castelli
Department of Mechanical Engineering
Columbia University
New York, New York 10027

Professor H. Elrod
Department of Mechanical Engineering
Columbia University
New York, New York 10027 (2)

Mr. Gerald B. Speen
Division Manager
Conductron
P. O. Box 844
Northridge, California 91324

Mr. J. W. Lower, Chief
Engineer-Inertial Components
Honeywell Aero Division
2600 Ridgeway Road
Minneapolis, Minnesota 55455

Mr. J. Levine
Ford Instrument Company
31-10 Thomson Avenue
Long Island City, New York 11101

Mr. Schuyler Kleinhans
Vice President - Engineering
Douglas Aircraft Company, Inc.
Santa Monica, California 90406

Engineering Societies Library
345 East 47th Street
New York, New York 10017

Library & Information Services
General Dynamics-Convair
P. O. Box 1128
San Diego, California 92112

Dr. John E. Mayer, Jr.
Research and Engineering Center
Ford Motor Company
P. O. Box 2053
Dearborn, Michigan 48123

Professor D. D. Fuller
Laboratories for Research and Development
The Franklin Institute
Philadelphia, Pennsylvania 19104 (3)

Mr. Jerry Glaser
Senior Project Engineer (Dept 37)
AiResearch Manufacturing Division
The Garrett Corporation
9851 S. Sepulveda Boulevard
Los Angeles, California 90009

Library
General Atomic Division
General Dynamics Corporation
P. O. Box 608
San Diego, California 92112

Mr. G. R. Fox
Research and Development Center
General Electric Company
P. O. Box 8
Schenectady, New York 12381

Mr. C. C. Moore, Specialist
Advanced Bearing & Seal Technology
General Electric Company
Flight Propulsion Division
Cincinnati, Ohio 45215

Mr. E. Roland Maki
Mechanical Development Department
General Motors Corporation
12 Mile and Mound Roads
Warren, Michigan 48090

Mr. Howard F. Traeder
Instruments Engineering Department
AC Electronics Division
General Motors Corporation
Milwaukee, Wisconsin 53201

Mr. Walter Carow
Kearfott Division
General Precision Incorporated
1150 McBride Avenue
Little Falls, New Jersey 07425

W. David Craig, Jr.
Mechanical Design Section
Grumman Aircraft Engineering Corporation
Bethpage, Long Island, New York 11714

Mr. P. Eisenberg, President
Hydronautics, Incorporated
Pindell School Road
Howard County
Laurel, Maryland 20810

Professor L. N. Tao
Illinois Institute of Technology
Chicago, Illinois 60616

Mr. Stanley Abramovitz, Director
Industrial Tectonics, Inc.
Fluid Film Bearing Division
New South Road and Commercial Street
Hicksville, Long Island, New York 11803

The Johns Hopkins University
Applied Physics Laboratory
8621 Georgia Avenue
Silver Spring, Maryland 20910
Attn: Fenton L. Kennedy
Document Library

Lockheed Missiles and Space Company
Technical Information Center
3251 Hanover Street
Palo Alto, California 94301

Dr. J. S. Ausman
Litton Systems, Inc.
5500 Canoga Avenue
Woodland Hills, California 91364 (2)

Mr. Don Moors
Litton Systems
5500 Canoga Avenue
Woodland Hills, California 91364 (2)

Library
The Marquardt Corporation
16555 Saticoy
Van Nuys, California 91409

Massachusetts Institute of Technology
Instrumentation Laboratory
68 Albany Street
Cambridge, Massachusetts 02139
Attn: Library, ILI-109

Professor Herbert H. Richardson
Room 3-461
Massachusetts Institute of Technology
Cambridge, Massachusetts 02139

McDonnell Aircraft Corporation
Post Office Box 516
St. Louis, Missouri 63166
Attn: Library, Dept. 218

Dr. Beno Sternlicht
Mechanical Technology Incorporated
968 Albany-Shaker Road
Latham, New York 12110

Mr. Carl F. Graesser, Jr.
Director of Research
New Hampshire Ball Bearings, Inc.
Peterborough, New Hampshire 03458

Professor A. Charnes
The Technological Institute
Northwestern University
Evanston, Illinois 60201

Mr. E. L. Swainson, Chief of Research
Precision Products Department
Nortronics
A Division of Northrop Corporation
100 Morse Street
Norwood, Massachusetts 02062

Northrop Norair
3901 West Broadway
Hawthorne, California 90250
Attn: Tech. Info. 3343-32

Professor P. R. Trumpler
Towne School of Civil and Mechanical Engineering
University of Pennsylvania
Philadelphia, Pennsylvania 19104

Pratt & Whitney Aircraft
Division of UAC - CANEL
P. O. Box 611
Middletown, Connecticut
Attn: Librarian

Radio Corporation of America
Camden, New Jersey 01802
Attn: Library, Building 10-2-5

Mr. Robert S. Siegler
Rocketdyne
Nucleonics Subdivision
6633 Canoga Avenue
Canoga Park, California 91304 (1)

Mrs. Florence Turnbull
Engineering Librarian
Sperry Gyroscope Company
Great Neck, New York 11020

W. G. Wing
Sperry Gyroscope Company
2T120
Great Neck, New York 11020

R. G. Jordan
Oak Ridge Gaseous Diffusion Pl.
Union Carbide Corp. Nuclear Div.
P. O. Box P
Oak Ridge, Tennessee 37830

Ralph F. DeAngelias, Technical Librarian
Norden Division of United Aircraft Corporation
Helen Street
Norwalk, Connecticut 06852

Mr. J. M. Gruber, Ch. Engrg.
Waukesha Bearings Corporation
P. O. Box 798
Waukesha, Wisconsin 53186

John Boyd
Westinghouse Research Laboratories
Churchill Boro
Pittsburgh, Pennsylvania 15235

Mr. H. Walter
Vice President - Research & Development
Worthington Corporation
Harrison, New Jersey 07029

Dr. Galus G. Goetzel, D/52-30
Bldg. 201, Plant 2, Palo Alto
Lockheed Missiles & Space Company
P. O. Box 504
Sunnyvale, California 94086

Mr. Philip J. Mullan
Staff Engineer - Advanced Tapes
IBM Data Systems Division
Development Laboratory - Box 390
Poughkeepsie, New York 12602

Science & Technology Division
Library of Congress
Washington, D. C. 20540

Admiralty Compass Observatory
Ditton Park
Slough, Bucks, England
Attn: Mr. Henri J. Elwertowski

The University of Southampton
Department of Mechanical Engineering
Southampton, England
Attn: Dr. H. S. Grassam

The Bunker-Ramo Corporation
Attn: Technical Library
8433 Fallbrook Avenue
Canoga Park, California 91804

Research Committee in Information
The American Society of Mechanical Engineers
345 East 47th Street
New York, New York 10017

Supervisor, Tech. Library Section
Thiokol Chemical Corporation
Wasatch Division
Brigham City, Utah 84302

Mr. Alfonso Alcedan L., Director
Laboratorio Nacional De Hydraulics
Ant iguo Cameno A. Ancon
Casilla Jostal 682
Lima, Peru

National Research Council
Aeronautical Library
Attn: Miss O. M. Leach, Librarian
Montreal Road
Ottawa 7, Canada

Professor J. K. Lunde
Skipsmodelltanken
Trondheim, Norway

Dr. Charles C. W. Ng
IIT Research Institute
10 West 35th Street
Chicago, Illinois 60616

Mr. I. C. Weymouth
Massachusetts Institute of Technology
Instrumentation Laboratory
275 Massachusetts Avenue
Cambridge, Massachusetts 02139

Mr. Sherrill Hisaw
The LaFleur Corporation
16659 South Gramercy Place
Torrance, California

Mr. Edgar J. Gunter, Jr.
University of Virginia
School of Engineering and Applied Science
Charlottesville, Virginia 22903

Mr. J. Licht
Department of Mechanical Engineering
Columbia University
New York, New York 10027

Mr. R. A. Minard
Assistant Product Manager
Gas Bearing Technology Division
MPB Incorporated
Precision Products Division
Keene, New Hampshire

Professor J. Modrey
Department of Mechanical Engineering
Purdue University
Lafayette, Indiana

Mr. J. W. Kannel
Battelle Memorial Institute
505 King Avenue
Columbus, Ohio 43201